

Andrzej Pożarycki

Dr inż.

Instytut Inżynierii Lądowej Politechniki Poznańskiej

andrzej.pozarycki@put.poznan.pl

Tomasz Moralewski

Hax HYDRAULICS, Hax Warias Dariusz

tmoralewski@hax-serwis.pl

Mariusz Wesolowski

Ppłk dr inż.

Instytut Techniczny Wojsk Lotniczych, Zakład Lotniskowy, Warszawa

mariusz.wesolowski@itwl.pl

DOI: 10.35117/A_ENG_18_12_07

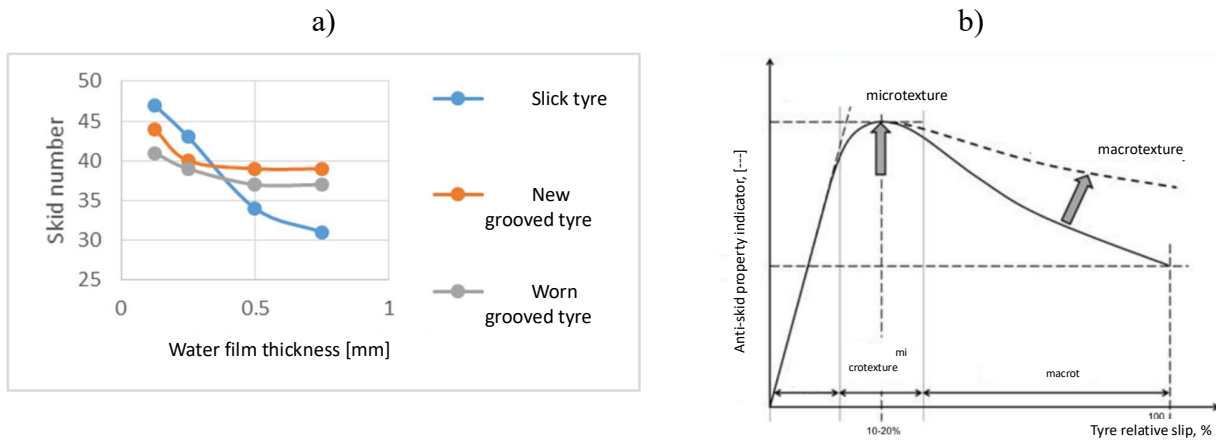
Skid resistance properties of airport pavements using a device with artificially enforced vertical pressure

Abstract: In the measuring systems for determining the skid resistance properties of airport pavements, the concept of artificially enforced vertical pressure dominates among a number of solutions. This is a natural choice considering the real contact conditions that prevail during aircraft starting and landing maneuvers. The article describes the consequences of shaping mechanical systems that induce vertical pressure of the measuring wheel to the pavement surface. The analysis was supported by a set of test results of anti-slip properties of airport pavements. As a result, the statistical aspects of the value of the vertical downforce are presented in the context of variable conditions determining the properties of the surface layer of the surface.

Keywords: Skid resistance; airport pavements

Introduction

The number of available solutions and the variety of individual methods for marking skid resistance properties of the pavements makes the obtained values, e.g. of pavement grip indices to be unique for individual devices. Examples of dependencies, which depict the variability of a sample pavement skid resistance index due to adopted technical parameters of a measuring system are shown, among others, in figure 1, relative to the “skid number” parameter as per standard ASTM E - 274.

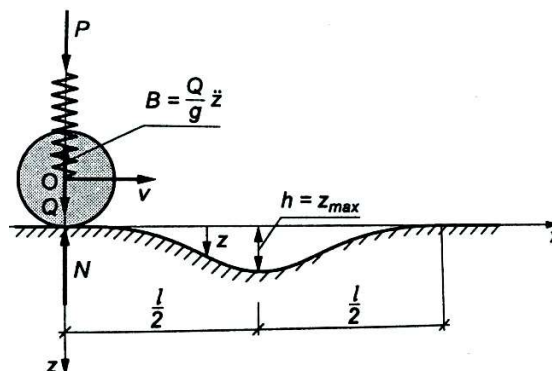


1. Illustration of typical changes of the pavement skid resistance index in the function of: a) different test tyre types [2], b) depending on the relative tyre skid number [7]

This is why, when deciding to diagnose the pavement skid resistance properties, try to select methods, which guarantee access to all values generated by the measuring system sensors during the tests. After all, the result of a high number of variables [1],[3],[4], which accompanies the phenomena occurring at the interface between a tyre and a pavement surface layer is that there are no universal methods around the world, which could be used to convert the results of pavement measurements, conducted with various devices. This is one of the reasons, why the pavement skid resistance property evaluation criteria are different for each of the devices. In terms of airfield pavements, the criteria are summarized for several devices approved by the International Civil Aviation Organization (ICAO) and in relation of road pavements, the criteria defined for SRT devices are applicable.

Objective

If a measuring wheel moves along a horizontal, rigid track, the pressure on the track is a static pressure and in reference to figure 2, it can be calculated as $N_{st.} = P + Q$.



2. Model of wheel elastic movement along a rigid track (no skid)

In the event of an unevenness under the wheel, it begins to move not only horizontally but also vertically, with acceleration \ddot{z} . If we assumed that unevenness are described by a curve equation in the form:

$$z = \frac{h}{2} \left(1 - \cos\left(\frac{2\pi x}{l}\right)\right) \quad 1)$$

than for $x = 0$, minimum N value is (2):

$$N_{min} = P + Q \left(1 - \frac{2\pi^2 v^2 h}{gl^2}\right) \quad 2)$$

and for $x = l/2$, N value reaches a maximum equal to (3):

$$N_{min} = P + Q \left(1 + \frac{2\pi^2 v^2 h}{gl^2}\right) \quad 3)$$

From the point of view of measuring skid resistance properties (e.g. friction coefficient), it should be noted that with a satisfied unevenness $\frac{2\pi^2 v^2 h}{gl^2} > 1$, the dynamic pressure force value can be lower than the value of force P. This means that when measuring on a pavement with specific combination of longitudinal unevenness parameters and measurement speed, the wheel detaches from the track.

In the light of the above, the objective of the research paper is to present actual and non-filtered distributions for values, which are used to calculate the grip index with the use of equations with artificially induced and controlled vertical pressure of the wheel to the pavement. In addition, it is assumed that the measurements are taken on pavements with the longitudinal unevenness index value meeting the condition $IRI < 3$.

Measurement methodology

The measurements involved using a CSR device [5],[6] which was constructed as an output of cooperation between industrial (HAX) and scientific (Poznan University of Technology) units, with the participation of a research team from the Air Force Institute of Technology during comparative studies.



3. View of a device constructed for the purposes of determining the grip index of airfield pavements.

The evaluation of pavement skid resistance properties in a CSR device was based on a standard model (4) used to estimate the friction index for the tyre/pavement interface, expressed with the CSR_i (Continuous Skid Resistance index) relationship.

$$CSR_i = \frac{M}{F \cdot r} \quad (4)$$

where:

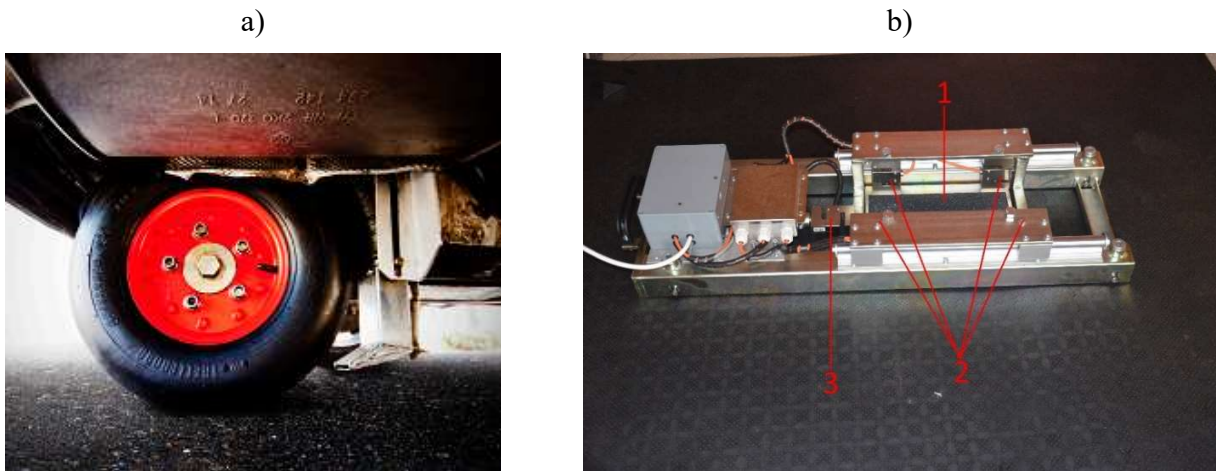
CSR_i – longitudinal grip index, [-]

M – recorded torque value, [Nm]

F – recorded value of the tyre-pavement vertical pressure force, [N]

r – torque arm, [m] (in static conditions equal to 0.21 m).

In relation to the characteristics shown in figure 1b, the CSR device used a measuring wheel slowed down relative to the device wheels by 13%. During a passage of the device, the CSR_i is determined every 10 cm. Hence, a user has the option to conduct a conventionally continuous measurement of road pavement skid resistance properties. A Unitester 520 tyre was used for the measurements, and the tyre pressure of 700 kPa (7 bar). The measurements were conducted both in “dry”, as well as “wet” conditions, using a 1mm thick water film (figure 4a). In order to monitor the conditions, the device is equipped with an instrument for periodic, static calibration of tensometric transducer. The following values are also monitored: vertical force and torque, which are compared with the reference values of tensometric transducer of a calibration stand shown in figure 4b.

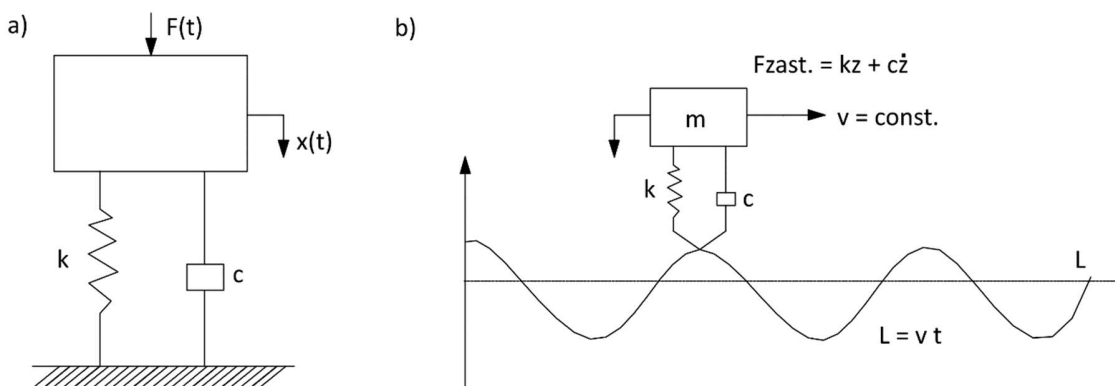


4. View, from left to right: a) measuring wheel with a water supply nozzle, b) static calibration stand for tensometric transducers installed on a CSR device (1- place for a measuring wheel tyre (sliding table) 2 and 3 – tensometric force transducers for calibrating the vertical force and torque, respectively)

The calibration procedure involves: 1) positioning the stand under the CSR device measuring wheel tyre, 2) lowering the measuring wheel and applying a pressure force with a value of ≤ 1400 N, 3) reading the value obtained on reference transducers, 4) inducing sliding of the torque calibration table, 5) reading the torque value, assuming that the force application arm is constant, 6) the values being recorded by a CSR device on-board computer, 7) comparing the readings and, if sensor indications differ by more than 5%, introducing calibration changes.

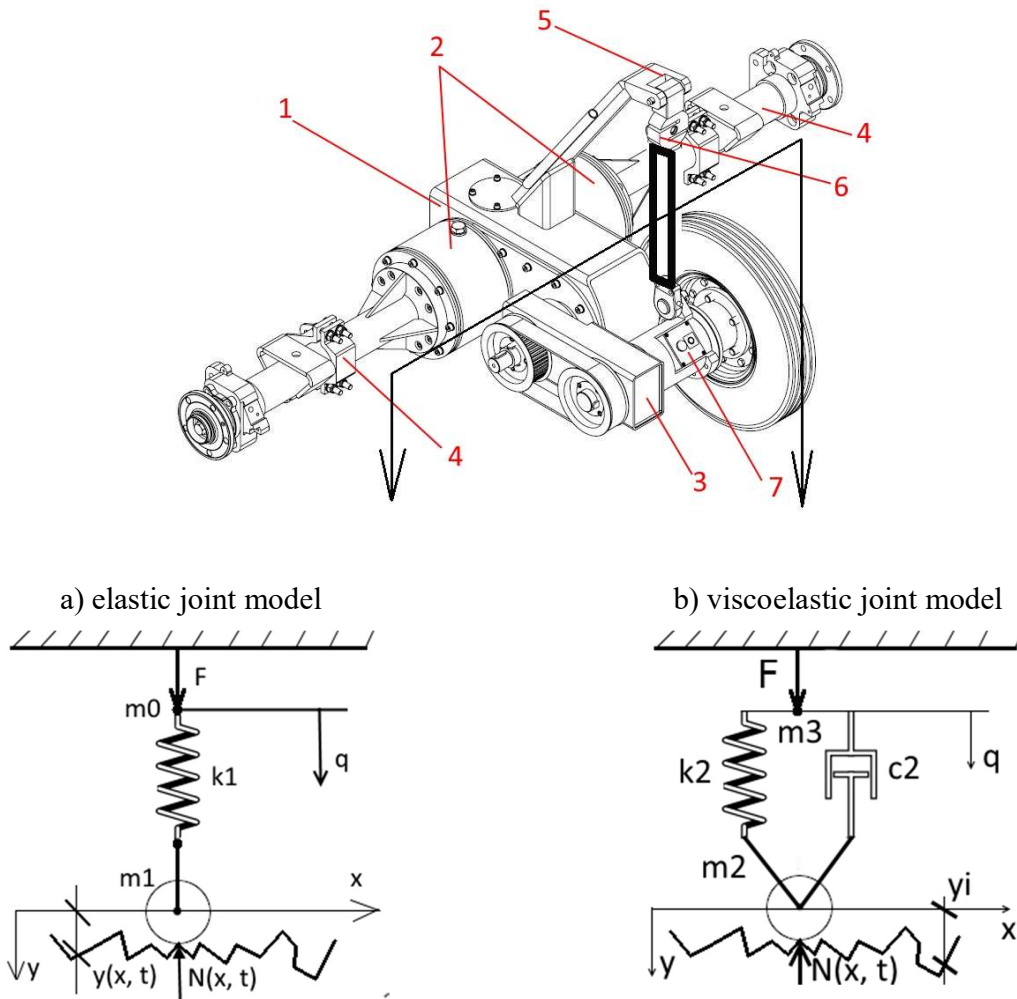
Characteristics of a measuring wheel dynamic model

In the case of the solution shown in figure 3b, the issue of analysing model properties (4) can be linked with the analysis of kinematic input [2]. The impact of pavement unevenness is then determined by a model, which describes the measuring wheel response to an externally applied movement along a rigid track. Generally, the diagrams for models with force and kinematic inputs are shown in figure 5.



5. The illustration shows input equivalence in a system with one degree of freedom a) force input, b) kinematic input

A diagram of the solutions in question, which interfere with the scope of the mechanical structure of the CSR device rear axle is shown in figure 6, where 1) toothed gear, 2) coupling chambers, 3) rocker with measuring wheel, 4) semi-axle assembly, 5) hydraulic cylinder fastening, 6) force tensometric transducer, 7) torque tensometric transducer. Results for the solutions of the measuring wheel-pavement downforce are shown in a system with one degree of freedom but applying the concept of the models with an elastic (figure 6a) and visco-elastic (figure 6b) link.



6. Diagrams of tested measuring system models for a CSR device

The consequence of enforcing all kinds of loads on the tyre-pavement interface during grip index measurements is a different character of the model (4), which in the context of solutions shown in figure 6a and 6b, takes the form of (5) or (6), respectively.

$$CSR_i = \frac{M}{N(x,t) \cdot r}, \text{ where } N(x, t) = F + m_1 g - m_1 \ddot{y} - m_0 \ddot{q} \quad (5)$$

where (designations in accordance with figures 6a and b):

$$m_0 \ddot{q} + k_1(q - y) = 0 \text{ and } m_1 \ddot{y} - k_1(q - y) - (m_0 + m_1)g = 0$$

$$\text{CSR}_i = \frac{M}{N(x,t) \cdot r}, \text{ where } N(x, t) = F + m_2 g - m_2 \ddot{y} - m_3 \ddot{q} \quad (6)$$

where (designations in accordance with figures **6a** and **b**):

$$m_3 \ddot{q} + c_2(\dot{q} - \dot{y}) + k_2(q - y) = 0 \text{ and } m_2 \ddot{y} - c_2(\dot{q} - \dot{y}) - k_2(q - y) - (m_3 + m_2)g = 0$$

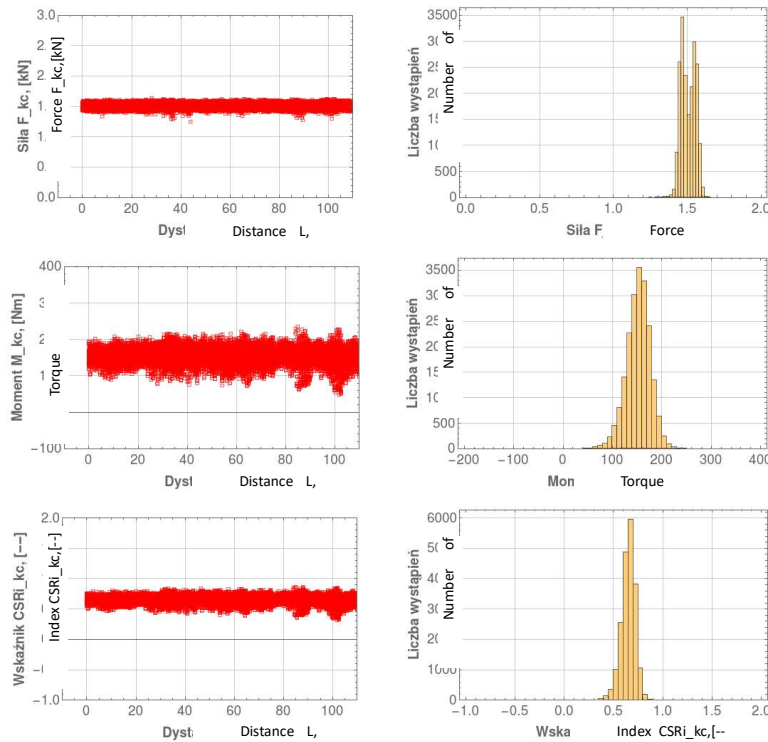
The behaviour of individual solutions models is shown on the example of results obtained in measuring campaigns described in the further part of this elaboration.

Measurement results

The measurements were taken on a runway with an asphalt pavement and a cement concrete parking pavement. The measurement sections were 100 metres long in each case. The complete set of results in the course of the measuring campaigns includes the following scenarios:

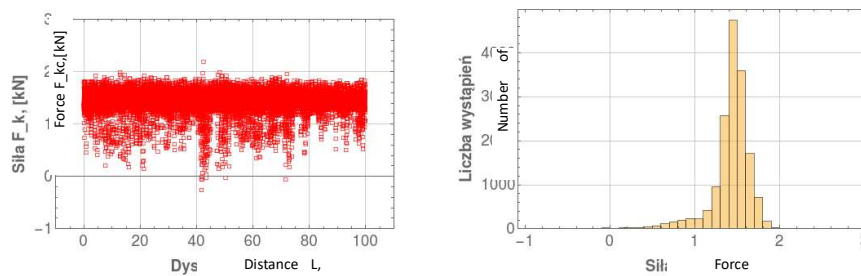
- measurements on an SMA 0/11 mm asphalt concrete pavement section ("dry" and "wet" measurement); IRI value < 1,5;
- measurements on a cement concrete pavements with burlap mat ("dry" and "wet" measurement); IRI value < 3;

The Spring-time measurements involves the model shown in figure **6a**, while the Summer-time measurements used the one shown in figure **6b**. In consequence, the analysis of a single pavement section included 19900 measurement results. Figures 7 and 8 show the impact of longitudinal unevenness on recorded values of the vertical force and torque. In the first case, the graphs show measurement results on the runway, at a speed on 65 km/h and in "wet" conditions. Whereas, figure 8 shows the actual response of the system to analogous measurement results but for a cement concrete pavement section.



8. Measurement results for a runway with a wearable asphalt surface ($v = 65 \text{ km/h}$, “wet”, used solution model in the CSR device - as per figure 6b)

For comparison, figure 9 also shows the response of the measuring wheel-pavement vertical downforce obtained during the measurements of a cement concrete pavement, at a speed of 65 km/h and without creating a water film.

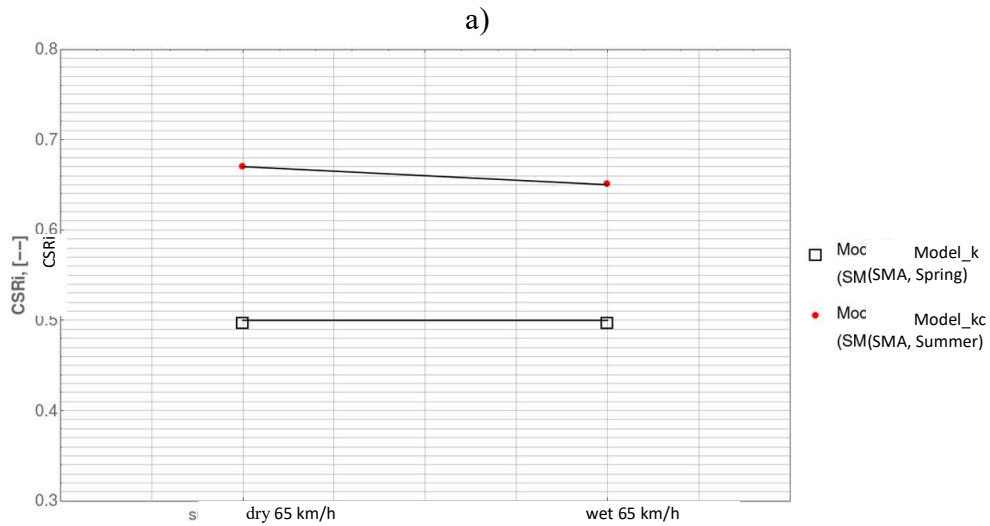


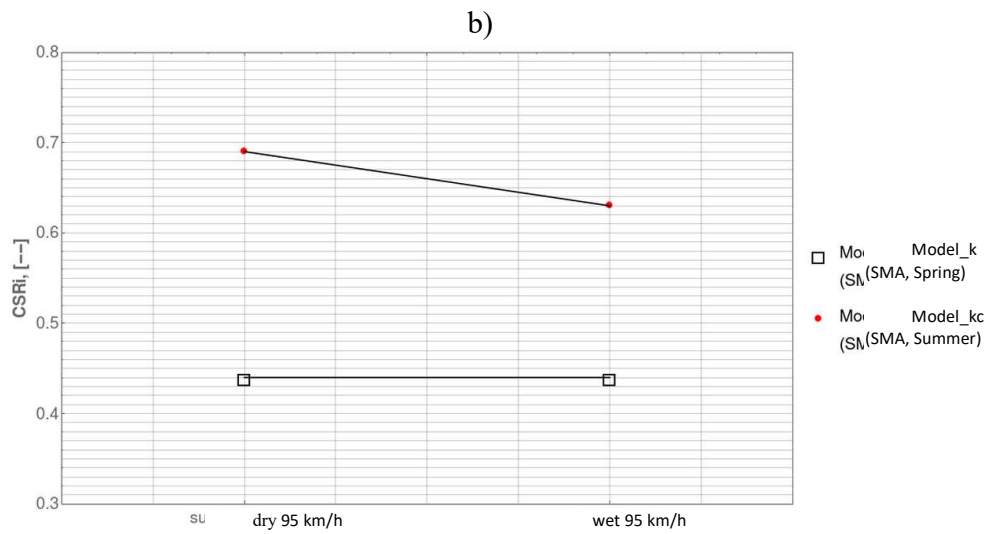
9. Graph of the measuring wheel-pavement vertical downforce together with a histogram for cement concrete pavement “wet” measurements, at a speed of 65 km/h (solution model - as per figure 6a)

The analysis of force values listed in figure 9 indicates that a model with an elastic solution (figure 6a) is so sensitive that the phenomenon of the measuring wheel detaching from the track occurs. This means that the pavement longitudinal evenness factors and the force of inertia consequently lead to different values of the grip index values obtained for both tested models.

Discussion

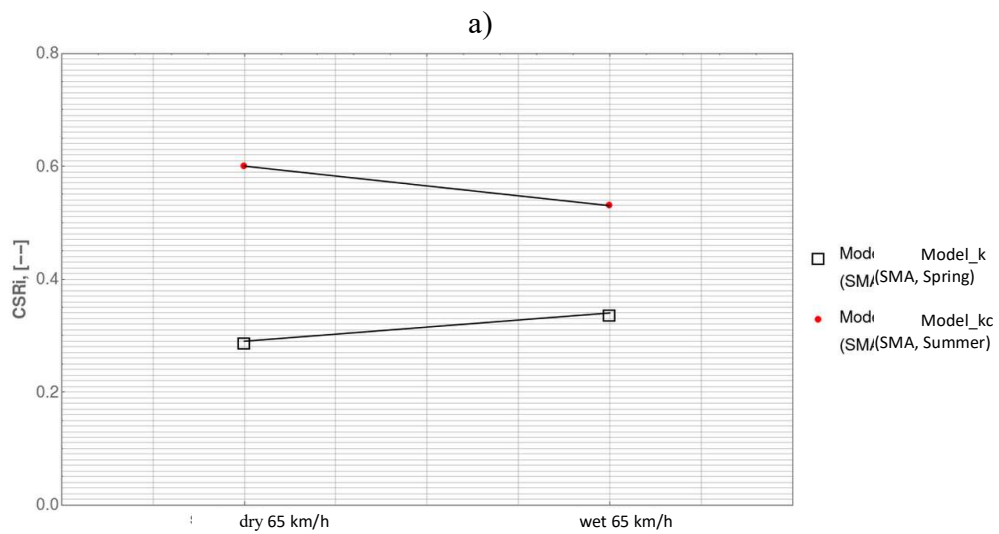
Comparing the absolute values of CSRI obtained with the use of both solutions discussed in the article, due to different approaches towards the shape of a measuring wheel-pavement vertical downforce cannot be taken into account in this case. However, it is possible to track the response of these two measuring systems to changing measurement conditions. Figures **10a** and **b** show the response of both solutions on the example of measurement results for an asphalt pavement.

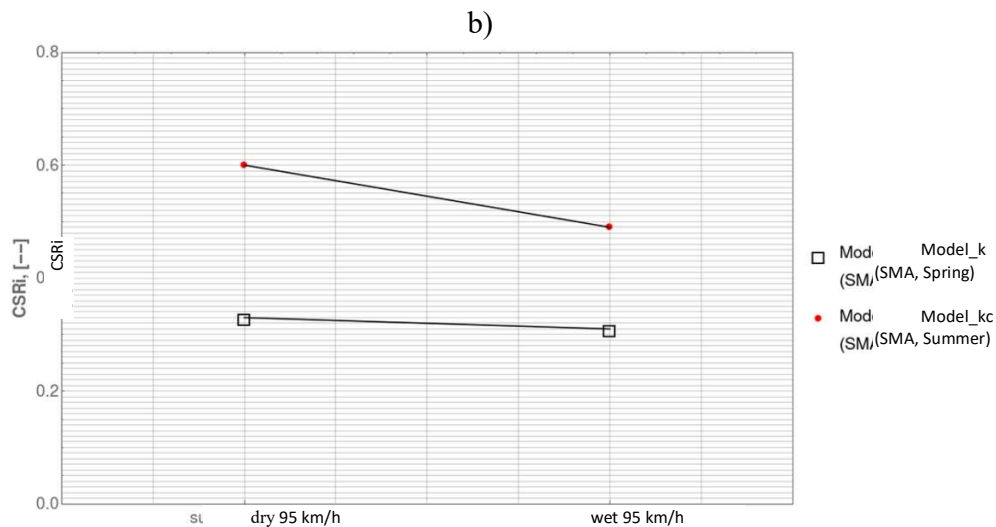




10. Graphic presentation of a measuring system response in “dry” and “wet” measurements on a asphalt pavement: a) measurement speed 65 km/h and b) measurement speed 95 km/h

By analogy to the results shown in figure 10, the response for an elastic and viscoelastic model is shown in figures 11a and b.





11. Graphic presentation of a measuring system response in “dry” and “wet” measurements on a cement concrete pavement: a) $v = 65$ km/h and b) $v = 95$ km/h

A characteristic feature of the solution with an elastic model is the measuring system response to the use of a water film and measurements without the film. A user generally expects that the grip index value will be lower both along with increasing measurement speed, as well as in “wet” conditions, compared to the measurements without water. In the case of this experiment, these principles are confirmed for the results obtained when using a model with a damper.

Conclusions

The research paper discusses the results of an experiment, which was conducted with the use of a CSR device, constructed for the purposes of determining longitudinal grip index of airfield pavements at various speeds. Attention was paid to recognizing the properties of measuring systems used in this device, which are determined mainly by the properties of an elastic and visco-elastic model. Based on the analysis of the result obtained during the measuring campaigns on two types of airfield pavements it was concluded that, as expected, a system of a model with a damper leads to two main conclusions, 1) statistical distributions developed for indirect values constituting the CSRI index model are much more centred around the mean value, relative to similar distributions for an elastic model, 2) a damper consistently reduced the unwanted impact of longitudinal evenness on the calculated CSRI values, limiting the tendency of a measuring system to record indirect values and detach the measuring wheel from the pavement.

Source materials

- [1] Burtos M., et. al. Development of correlation equations between different measurements of skid resistance in pavements. *Indian Journal of Engineering & Material Sciences*, Vol. 13, April 2006, pp. 117-122.
- [2] Cempel C. *Drgania mechaniczne - wprowadzenie. [Mechanical vibrations - Introduction]* Poznań University of Technology, 1982.
- [3] Descornet G., et. al. Harmonization of European Routine and research Measuring Equipment for Skid Resistance. FEHRL Report 2006/01, pp. 1-161.

-
- [4] International Experiment to Compare and Harmonize Skid Resistance and Texture Measurements. PIARC ,1995, 430 pages.
 - [5] Pożarycki A., Fengier J., Wyczałek M., Skrzypczak P., Wesołowski M., Blacha K., Analiza wyników metody fotogrametrycznej w świetle właściwości przeciwpoślizgowych nawierzchni [*Analysing the results of the photogrammetric model in the light of pavement skid-resistance properties*], Drogownictwo, 2017, vol. 3, pp. 75-84
 - [6] Pożarycki Andrzej, Fengier Jakub, Warias Dariusz, Tomasz Moralewski. Identyfikacja odcinków nawierzchni lotniskowych o zmiennych właściwościach przeciwpoślizgowych urządzeniem CSR [*Identification of airfield pavement sections with variable skid resistance properties using a CSR device*] Poznań - Lotnictwo dla obronności, Wydawnictwo Politechniki Poznańskiej, 2016, pp. 483-494.
 - [7] Ueckermann A., Wang D., Oeser M. and Sreinauer B. Towards Contactless Skid Resistance Measurement. Safer Roads International Conference, May 18-21, 2014, UK.